Colloid Polym Sci 275:106–115 (1997)

ORIGINAL CONTRIBUTION

P.A.M. Steeman
J. van Turnhout

A numerical Kramers–Kronig transform for the calculation of dielectric relaxation losses free from Ohmic conduction losses

Received: 17 May 1996
Accepted: 16 August 1996

Dr. P.A.M. Steeman (✉)
DSM Research B.V.
P.O. Box 18
6160 MD Geleen, The Netherlands

J. van Turnhout
Technical University Delft
Department of Polymer Technology
P.O. Box 5045
2600 GA Delft, The Netherlands

Abstract A numerical Kramers–Kronig transform is described which allows the calculation of dielectric relaxation losses from dielectric constant data measured at a limited set of frequencies differing by a factor of 2. Conversion formulas for both the central frequencies and for frequencies near the edges of the experimental frequency window are derived. The approach used can be extended easily to measurement frequencies with a different logarithmic spacing.

Using this conversion, relaxation and dissipative, conduction losses can be separated. In this way Ohmic conduction processes and simultaneously occurring relaxation processes like dipole or space-charge relaxations can be analysed independently. The results of some simulations and of calculations on experimental data for poly(vinyl-chloride) are used to illustrate the potentials of the ε' to ε'' conversion.

Key words Dielectric spectroscopy – ε' to ε'' conversion – relaxation loss – Ohmic conduction – space charge relaxations – interfacial polarization – polymer – poly(vinyl-chloride) – numerical KK-transform

Introduction

The study of the dielectric properties of materials is often hampered by dissipative losses due to Ohmic conduction. In studying polymeric materials this situation is encountered at temperatures above the glass transition. Since Ohmic conduction losses show a reciprocal dependence on frequency, this problem is the most pronounced when low measuring frequencies are used. Moreover, it is well-known that a special class of relaxation mechanisms, the so-called space-charge and interfacial or Maxwell–Wagner–Sillars processes [1–3] occur only when the material under study is electrically conductive. By studying these mechanisms, for example, in heterogeneous materials, often detailed morphological information can be obtained [4–6]. In such cases it would be advantageous if conduction and relaxation mechanisms could be separated. Many authors [7–9] perform this separation by fitting a $1/\omega$ curve to the measured dielectric loss, because in this way the Ohmic conduction losses can be approximated. However, if pronounced interfacial or space-charge losses are present, the accuracy of this approach is limited, especially when the exact shape of the relaxation loss curve is sought for.

It is well-known that the Kramers–Kronig relations offer a tool for performing an exact analysis. These equations state that the relative dielectric constant $\varepsilon'(\omega)$ and dielectric loss $\varepsilon''(\omega)$ are related through integral equations:

$$\varepsilon''(\omega_0) = \frac{\sigma_{dc}}{\varepsilon_v \omega_0} + \frac{2}{\pi} \int_0^\infty \varepsilon'(\omega) \frac{\omega_0}{\omega^2 - \omega_0^2} d\omega \quad (1)$$

$$\varepsilon'(\omega_0) = \varepsilon_\infty + \frac{2}{\pi} \int_0^\infty \varepsilon''(\omega) \frac{\omega}{\omega^2 - \omega_0^2} d\omega \quad (2)$$

in which ω is the angular frequency [rad/s], ε_v the permittivity of vacuum (8.82 pF/m), σ_{dc} [S/m] the Ohmic

conductivity of the material and ε_∞ the high frequency relative dielectric constant of the material.

Note that pure Ohmic conduction does not contribute to the dielectric constant. Therefore, the integral term in Eq. (1) equals the relaxation losses searched for, while the first term pertains to the Ohmic conduction losses. Thus, if the relaxation losses are obtained by transforming the dielectric constant data using (1), the Ohmic conduction losses can be calculated by subtracting the polarization loss from the actual measured loss.

In practice, the use of these equations is not straightforward since dielectric data over a wide range of frequencies are required. Moreover, the singularity of the integral kernels at $\omega_0 = \omega$ makes it difficult to approximate the integrals numerically with a high precision.

From the work of Brather [10] and earlier work by Schwarzl [11] and Ferry and Ninomya [12] on mechanical relaxations, it is known that the integral equations can be approximated accurately by taking weighted differences of the dielectric constant or dielectric loss data at geometrically spaced frequencies. Brather gives accurate approximations for both the dielectric constant and the dielectric loss. Unfortunately, a rather broad range of frequencies is required for these calculations. Moreover, for data at frequencies near the edges of the experimentally accessible frequency window no approximations are given. It is the purpose of this work to introduce approximations which require only a limited set of frequencies to be available, both for central frequencies and for frequencies near the upper and lower end of the measuring range.

The numerical transform

The basic idea is to calculate the dielectric loss by weighted differences of dielectric constant data, using the following approximation:

$$\varepsilon''(\omega) \approx \sum_{i=1}^{n} b_i \cdot [\varepsilon'(\omega/2^i) - \varepsilon'(\omega * 2^i)] \,. \tag{3}$$

In order to limit the number of frequencies needed to calculate the relaxation losses we focused on $n = 4$. The relaxation behaviour of the dielectric constant $\varepsilon'(\omega)$ and the dielectric loss $\varepsilon''(\omega)$ of most polymers can be described by:

$$\varepsilon'(\omega) - \varepsilon_\infty = \Delta\varepsilon \int_0^\infty f(\tau) \frac{1}{1+\omega^2\tau^2}\, d\tau \tag{4}$$

$$\varepsilon''(\omega) = \Delta\varepsilon \int_0^\infty f(\tau) \frac{\omega\tau}{1+\omega^2\tau^2}\, d\tau + \frac{\sigma_{dc}}{\varepsilon_{vac}\omega} \tag{5}$$

where $\Delta\varepsilon = \varepsilon_s - \varepsilon_\infty$, with ε_s the static dielectric constant and $f(\tau)$ the distribution function. If only the relaxation losses are considered (as given by the first term in Eq. (5)) then equating the kernels of Eqs. (4) and (5) results in view of Eq. (3) in:

$$\sum_{i=1}^{n} b_i \cdot \left[\frac{4^i}{4^i+\omega^2\tau^2} - \frac{1}{1+4^i\omega^2\tau^2}\right] \approx \frac{\omega\tau}{1+\omega^2\tau^2} \,. \tag{6}$$

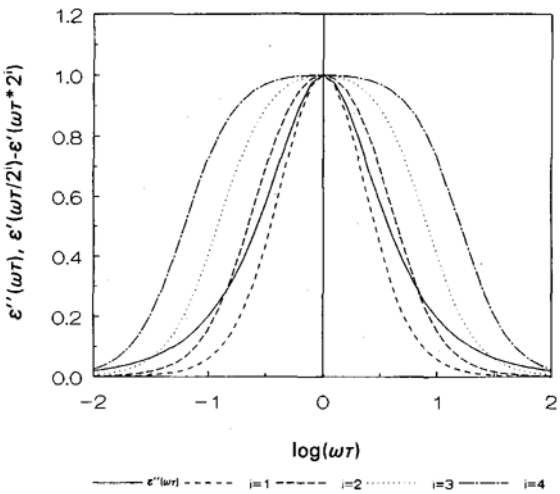

Fig. 1 The normalized kernels of Eq. 6 as a function of $\omega\tau$

Figure 1 illustrates how the integral kernel of the dielectric loss $\varepsilon''(\omega)$ can be approximated by a summation of a series of "loss curves" of varying width derived from dielectric constant differences according to Eq. (3). It can be seen from this figure that the ε'-difference kernel for $i = 1$ is a sharper function of $\omega\tau$ than the kernel of the dielectric loss, while the kernel with $i = 2$ has a comparable width. With increasing index i the ε'-difference kernels become broader and can be used for approximating the tails of the dielectric loss kernel.

The b_i coefficients which give the best fit for the approximation in Eq. (6) were obtained with a least squares analysis over the interval $10^{-1.5} < \omega\tau < 10^{1.5}$, using 50 data points per decade. In order to increase the accuracy of the fit near the edges ($\omega\tau \gg 1$ and $\omega\tau \ll 1$), we weighed the different terms in the least squares approximation with the reciprocal square of the dielectric loss kernel (i.e., we multiplied them with $\sqrt{\{(1+\omega^2\tau^2)/\omega\tau\}}$). Table 1 lists the b_i coefficients found.

By using only four differences, i.e., data over only +/− 1.2 decades of frequency, an accurate conversion, within a relative error of 4%, is obtained over the entire $\omega\tau$ interval mentioned. Beyond this interval the approximation underestimates the actual losses. For Debye type relaxation curves this is the most critical. In actual materials, the relaxation processes are broadened due to several interaction mechanisms [13]. In that case the description is quite accurate as will be demonstrated later. The limited

Table 1 The b_i ($i = 1, 2, 3, 4$) coefficients for the calculation of $\varepsilon''(\omega)$ from eight $\varepsilon'(\omega)$ data points

	central	edge 1	edge 2	edge 3
b_1	0.44530	0.92852	0.08725	1.08161
b_2	0.22726	− 0.42063	0.50708	− 0.64564
b_3	− 0.11000	0.33275	− 0.21489	0.38196
b_4	0.13458	0.00513	0.15248	0.01612

Table 2 The c_i ($i = 1, 2, 3, 4$) coefficients for the ε' to ε'' conversion using $-0.4\cdot\varepsilon''(\omega/2) + \varepsilon''(\omega) - 0.4\cdot\varepsilon''(2\omega)$

	central	edge 1	edge 2
c_1	0.50888	0.46975	0.42660
c_2	− 0.17575	− 0.13497	− 0.10012
c_3	0.02853	0.00888	− 0.00214
c_4	− 0.00417	− 0.00015	0.00123

range of frequencies required eliminates the need for a broad-band spectrometer, while we are still able to perform a satisfactory Kramers–Kronig conversion.

Edge formulas

Experimentally, a limited range of frequencies are available. The above discussed Eq. (3) can only be used if a geometric series of at least four lower and higher frequencies is available (i.e., $\omega/16 \ldots 16\omega$). This would seriously reduce the number of data points convertable by the Kramers–Kronig transformation. The problem occurs both at the lower and the upper end of the frequency interval. The simplest solution would be to reduce the number of terms (n) used to approximate the relaxation losses. This, however, would affect the accuracy of the approximation.

A better solution can be found by invoking additional half symmetrical differences, e.g., if $\omega/16$ is not available then use the difference $\varepsilon'(\omega) - \varepsilon'(16\omega)$, etc... Similarly, if 16ω is not available we use the difference $\varepsilon'(\omega/16) - \varepsilon'(\omega)$. In this way, an optimal use of the available data is made. For the lower frequencies, we use:

$$\varepsilon''(\omega) \approx \sum_{i=1}^{n_{max}} b'_i \cdot [\varepsilon'(\omega/2^i) - \varepsilon'(\omega * 2^i)] + \sum_{i=n_{max}+1}^{4} b'_i \cdot [\varepsilon'(\omega) - \varepsilon'(\omega * 2^i)] \quad (7)$$

and for the higher frequencies:

$$\varepsilon''(\omega) \approx \sum_{i=1}^{n_{max}} b'_i \cdot [\varepsilon'(\omega/2^i) - \varepsilon'(\omega * 2^i)] + \sum_{i=n_{max}+1}^{4} b'_i \cdot [\varepsilon'(\omega/2^i) - \varepsilon'(\omega)] \; . \quad (8)$$

The coefficients b'_i found for the edge equations are also listed in Table 1 (edge 1 for $n_{max} = 3$, edge 2 for $n_{max} = 2$ and edge 3 for $n_{max} = 1$). The coefficients for the sets of lower and upper frequencies are equal. For the highest and the lowest frequency ($n_{max} = 0$) no accurate approximations can be found.

Further optimization

In his work, Brather [10] showed that it is also possible to approximate a special combination of dielectric loss data in which the Ohmic conduction losses are cancelled:

$$-0.4\varepsilon''(\omega/2) + \varepsilon''(\omega) - 0.4\varepsilon''(2\omega) \; . \quad (9)$$

Since the contribution from Ohmic conduction to the dielectric loss is inversely proportional to the frequency ($\varepsilon''_{cond}(\omega) = \sigma_{dc}/\varepsilon_v\omega$) it can easily be seen that the conduction losses indeed cancel in the summation of Eq. (9).

The integral kernel of this equation can again be approximated with a sum of dielectric constant differences. Because this kernel is a sharper function of $\omega\tau$ it can be approximated even more accurately with a limited number of terms:

$$-0.4\varepsilon''(\omega/2) + \varepsilon''(\omega) - 0.4\varepsilon''(2\omega) \approx \sum_{i=1}^{n} c_i \cdot [\varepsilon'(\omega/2^i) - \varepsilon'(\omega * 2^i)] \; . \quad (10)$$

For the lower and the upper frequency edges equations similar to (7) and (8) were used. It was found that the approximation for edge 3 is poor and therefore omitted. The results of the least squares analysis are listed in Table 2.

From Table 2 it can be seen that only the symmetrical differences give a significant contribution; the asymmetrical differences can be omitted without introducing a serious error. Moreover, only the first three terms in the central approximation are significant, indicating that a narrower frequency spacing than the one used (e.g., factor $\sqrt{2}$ instead of a factor 2 spacing) would be profitable. Such an extension is straightforward.

The results from the direct approximation of $\varepsilon''(\omega)$ as discussed in the previous section can be used as a first guess to solve the set of conversions based on Eq. (10) iteratively. Two iterations then suffice. The iterative solution of Eq. (10) should be started preferably from the middle of the frequency range used, where the necessary starting values of ε'' as obtained from Eq. (3) are the most reliable.

Simulations

The accuracy of the numerical ε' to ε'' conversion was assessed by applying it to data generated with the Cole–Cole equation [14]:

$$\varepsilon^*(\omega) = \varepsilon'(\omega) - i\varepsilon''(\omega) = \varepsilon_\infty + \frac{\varepsilon_s - \varepsilon_\infty}{1 + (i\omega\tau)^\alpha} \qquad (11)$$

in which ε_s (was set to 2) and ε_∞ (also set to 1) are the static and the high frequency-limit values of the relative dielectric constant. The parameter α, with $0 \leq \alpha \leq 1$, is the so-called broadening parameter which determines the width of the relaxation curve along the frequency axis. $\tau[s]$ is the central relaxation time of the relaxation process and i the imaginary unit. For $\alpha = 1$ Debye type curves, the sharpest possible, are found. Usually, for polymeric materials α varies between 0.2 and 0.7 at most.

Tables 3–5 show the results of calculations on a Cole–Cole response with $\alpha = 0.6$, for three special cases: i) the maximum loss of the relaxation curve is centred in the available frequency interval (Table 3), ii) the maximum loss of the relaxation curve is in the lower half of the frequency interval (Table 4) and iii) the maximum loss arises at the lower edge of the interval (Table 5). The cases ii) and iii) are also illustrative when the maximum loss is situated in the upper end of the frequency range. Both the results obtained with the direct calculation of the dielectric loss using the Eqs. (3), (7) and (8) and the further optimization using Eq. (10) are given in these tables. During the simulations, the parameter ω/ω_0 was varied between 1/256 and 256, with $\omega_0\tau = 1, 10, 100$, respectively.

Table 3 The exact and the calculated dielectric loss for a Cole–Cole dispersion with $\alpha = 0.6$ and with its loss maximum at the centre ($\omega_0\tau = 1$)

ω/ω_0	$\varepsilon'(\omega/\omega_0)$ Cole–Cole	$\varepsilon''(\omega/\omega_0)$ Cole–Cole	$\varepsilon''(\omega/\omega_0)$ (3, 7, 8)	$\varepsilon''(\omega/\omega_0)$ (10)
1/256	1.979	0.028	–	–
1/128	1.967	0.041	0.037	–
1/64	1.950	0.060	0.057	0.058
1/32	1.923	0.087	0.083	0.085
1/16	1.883	0.122	0.120	0.120
1/8	1.823	0.164	0.162	0.162
1/4	1.738	0.207	0.206	0.206
1/2	1.628	0.241	0.241	0.241
1	1.500	0.255	0.254	0.254
2	1.372	0.241	0.241	0.241
4	1.262	0.207	0.206	0.206
8	1.177	0.164	0.162	0.162
16	1.117	0.122	0.120	0.120
32	1.077	0.087	0.083	0.085
64	1.050	0.060	0.057	0.058
128	1.033	0.041	0.037	–
256	1.022	0.028	–	–

Table 4 The exact and the calculated dielectric loss for a Cole–Cole dispersion with $\alpha = 0.6$ and an off-centre loss maximum at $\omega_0\tau = 10$

ω/ω_0	$\varepsilon'(\omega/\omega_0)$ Cole–Cole	$\varepsilon''(\omega/\omega_0)$ Cole–Cole	$\varepsilon''(\omega/\omega_0)$ (3, 7, 8)	$\varepsilon''(\omega/\omega_0)$ (10)
1/256	1.912	0.097	–	–
1/128	1.866	0.135	0.132	–
1/64	1.799	0.178	0.176	0.176
1/32	1.705	0.220	0.219	0.219
1/16	1.588	0.249	0.248	0.248
1/8	1.458	0.253	0.253	0.253
1/4	1.334	0.232	0.231	0.231
1/2	1.232	0.193	0.192	0.192
1	1.155	0.150	0.148	0.149
2	1.102	0.110	0.108	0.108
4	1.067	0.078	0.075	0.076
8	1.044	0.054	0.050	0.052
16	1.029	0.036	0.033	0.035
32	1.019	0.025	0.021	0.023
64	1.012	0.016	0.014	0.015
128	1.008	0.011	0.009	–
256	1.005	0.007	–	–

Table 5 The exact and the calculated dielectric loss for a Cole–Cole dispersion with $\alpha = 0.6$ with its loss maximum near the edge ($\omega_0\tau = 100$)

ω/ω_0	$\varepsilon'(\omega/\omega_0)$ Cole–Cole	$\varepsilon''(\omega/\omega_0)$ Cole–Cole	$\varepsilon''(\omega/\omega_0)$ (3, 7, 8)	$\varepsilon''(\omega/\omega_0)$ (10)
1/256	1.670	0.231	–	–
1/128	1.547	0.253	0.251	–
1/64	1.417	0.249	0.247	0.247
1/32	1.298	0.221	0.219	0.220
1/16	1.204	0.179	0.178	0.178
1/8	1.136	0.136	0.134	0.135
1/4	1.089	0.098	0.096	0.097
1/2	1.058	0.069	0.066	0.067
1	1.038	0.047	0.044	0.046
2	1.025	0.032	0.029	0.030
4	1.016	0.022	0.019	0.020
8	1.011	0.014	0.013	0.013
16	1.007	0.010	0.008	0.009
32	1.004	0.006	0.005	0.006
64	1.003	0.004	0.004	0.004
128	1.002	0.003	0.002	–
256	1.001	0.002	–	–

They clearly show the high accuracy obtained with the numerical transform. Use of Eq. (10) improves the predicted relaxation loss especially in the tails of the loss peak. Note that for the highest and the lowest frequency data accessed with Eq. (3) ($\omega\tau = 128$ and $\omega\tau = 1/128$), Eq. (10) cannot be used since that would require ε'' data at $\omega\tau = 256$ or $\omega\tau = 1/256$, which are not available from the ε'' data obtained with Eq. (3) that serve as initial guess.

Experimental results

In order to illustrate the application of the numerical Kramers–Kronig conversion to actual experimental data some results on poly(vinyl-chloride) which we reported recently [15] are discussed.

Dielectric measurements were performed on a compression moulded plate of poly(vinyl-chloride) with molar mass 65 kg/mol ($Kv = 80$ see [15]). The material was kindly supplied by Limburgse Vinyl Maatschappy (LVM), Belgium. Isothermal frequency scans were performed in the frequency range from 0.1 Hz to 10 MHz, with ten measurement frequencies per decade, thus including three nearly geometric data sets. The temperature was varied between 70° and 130 °C, with 5 °C intervals. The measurements were performed with a spectrometer built around a Schlumberger 1250 frequency response analyzer and a Hewlett Packard 4275A capacity-resistance (LCR) meter.

Figures 2 and 3 show the results of the isothermal frequency scans of the measured dielectric constant and the dielectric loss, respectively. In the dielectric loss curves the peaks of the α-relaxation arising from the dynamic glass-rubber transition, are clearly visible. With increasing temperature, the loss peaks shift strongly to higher temperatures. Meanwhile, a step-wise decrease in the dielectric constant from a level of about 12 down to about 3.5–4 is observed. At the lowest frequencies the dielectric loss shows a sharp increase with decreasing frequency, which is attributed to Ohmic conduction in the material, and which shows up in particular above the glass-transition temperature. The low frequency dielectric constant data

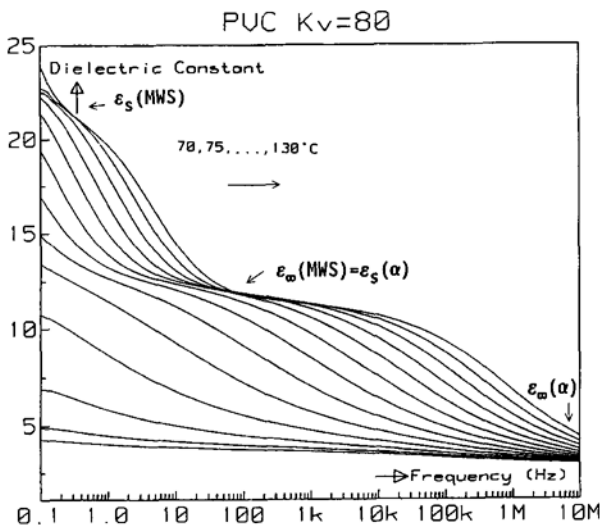

Fig. 2 The dielectric constant of PVC $Kv = 80$ as a function of frequency, at several temperatures

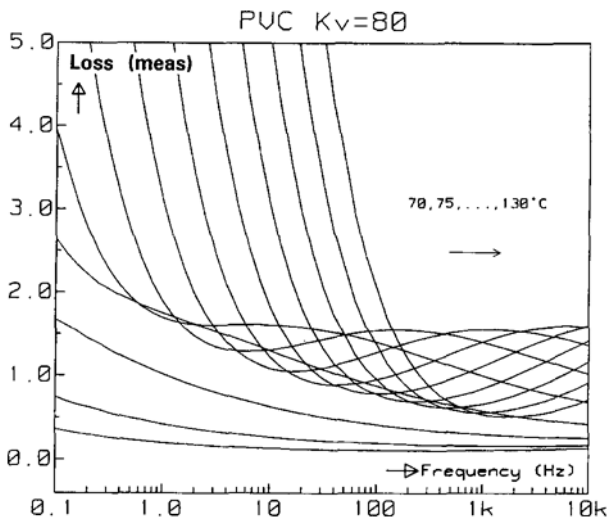

Fig. 3 The dielectric loss of PVC $Kv = 80$ as a function of frequency, at several temperatures

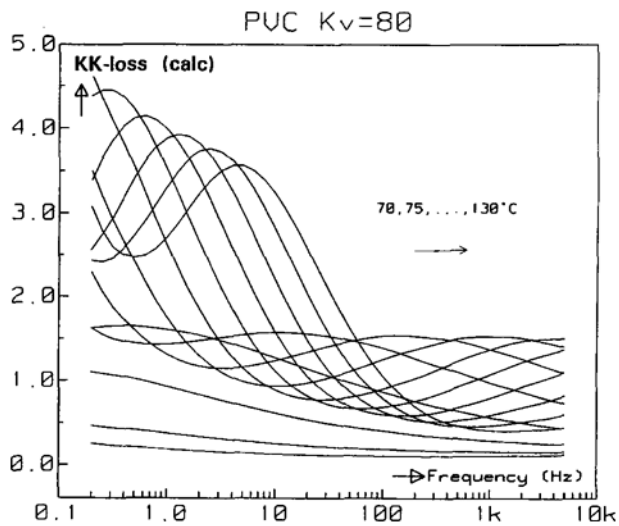

Fig. 4 The calculated relaxation loss of PVC $Kv = 80$ as a function of frequency, at several temperatures

indicate the presence of an additional relaxation process. However, the loss peaks of this process are not visible in the measured loss due to the high dissipative, conduction losses.

The numerical Kramers–Kronig transform was used to separate the conduction and the relaxation losses. Figure 4 shows the calculated relaxation losses. Now, the loss peaks of the low frequency relaxation process are clearly visible, and can be used for a quantitative analysis of this transition. The origin of this relaxation process was discussed in detail in [15]. It was shown to be an interfacial effect due to the processing conditions to which the sample was submitted (poor gelation). Note that the loss peaks of the α-transition, which show no overlap with the

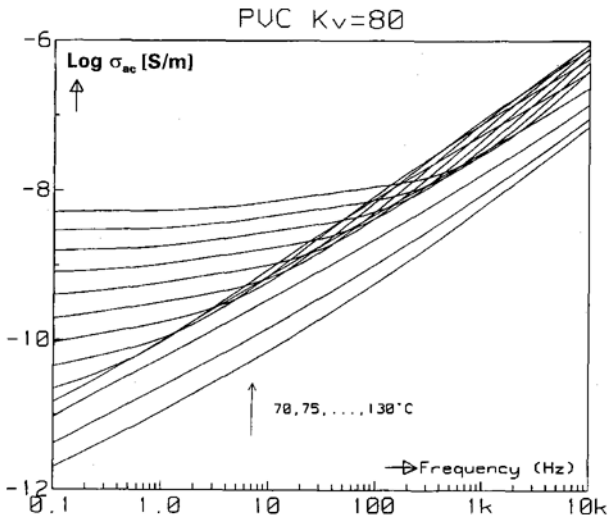

Fig. 5 The dynamic conductivity of PVC $Kv = 80$ as a function of frequency, at several temperatures

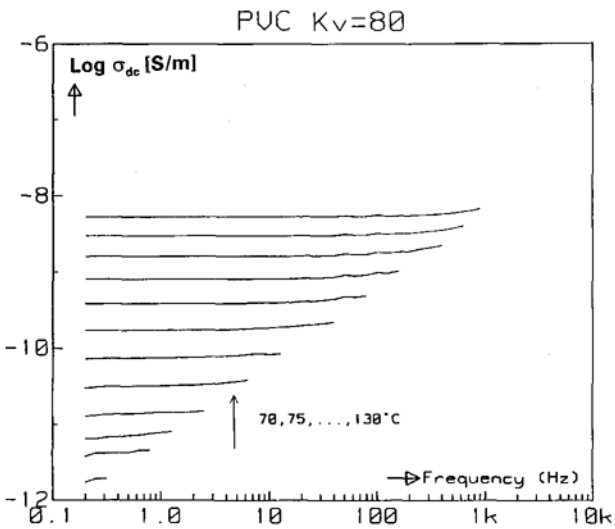

Fig. 6 The calculated Ohmic conductivity of PVC $Kv = 80$ as a function of frequency, at several temperatures

conduction process, are accurately predicted with the Kramers–Kronig transform. The Cole–Cole broadening parametersof the α-transition and of the low frequency transitions are about 0.4 and 0.7, respectively. For these values an accurate conversion with the transform can be expected.

Now the relaxation losses $\varepsilon''_{rel}(\omega)$ are known, the Ohmic or dc-conduction losses can be obtained by a simple subtraction:

$$\varepsilon''(\omega, T) = \frac{\sigma_{ac}(\omega, T)}{\varepsilon_v \omega} = \varepsilon''_{rel}(\omega, T) + \frac{\sigma_{dc}(T)}{\varepsilon_v \omega} \tag{12}$$

in which $\sigma_{ac}(\omega, T)$ [S/m] is the temperature and frequency dependent dynamic conductivity of the material which includes both the relaxation and the Ohmic conduction losses and which is derived directly from the measured dielectric loss $\varepsilon''(\omega)$ by multiplying it with ε_v and ω. $\sigma_{dc}(T)$ [S/m] is the temperature dependent (and frequency independent!) Ohmic conductivity of the material.

Figures 5 and 6 show the dynamic and Ohmic conductivity of the material, as a function of frequency, extracted at the various measuring temperatures. The Ohmic conductivity as plotted in Fig. 6 is indeed independent of frequency. At the lowest frequencies the dynamic and the Ohmic conductivity coincide, i.e., the dielectric losses then are dominated by the conduction process. By contrast, at higher frequencies the dynamic conductivity becomes dominated by the dipolar relaxation losses of the α-relaxation and is much higher than the dc-conductivity.

In evaluating the Ohmic conductivity as a function of temperature it could be shown [15] that the relaxation time of the low frequency relaxation process and the Ohmic conductivity are inversely proportional. This agrees with the assumption that free charge carriers (ions) are involved in this transition, which is typical for a space-charge or interfacial type of relaxation.

Conclusions

A numerical Kramers–Kronig transform is described which enables the calculation of the relaxation losses from the dielectric constant data using a limited range of geometrically spaced frequencies, even near the edges of the experimentally accessible frequency range. Data over about 2.4 decades of frequency can already be used for the analysis, thus eliminating the need for a broad band spectrometer.

The transformation can be applied advantageously in studying relaxation processes which cannot be determined directly due to high conduction losses, and which are often located at the lower frequency edge of the available experimental data. This is true, especially for interfacial or space-charge relaxation processes. Moreover, the conversion can be used to check the consistency of the dielectric constant and dielectric loss data acquired experimentally.

Appendix 1

Illustration of the use of the conversion formulaes

By inserting the coefficients from Table 1, we obtain for the conversion of ε'-data in the centre of the

frequency range:

$$\varepsilon''(\omega) = 0.44530*(\varepsilon'_{\omega/2} - \varepsilon'_{2\omega}) + 0.22726*(\varepsilon'_{\omega/4} - \varepsilon'_{4\omega}) - 0.11000*(\varepsilon'_{\omega/8} - \varepsilon'_{8\omega}) + 0.13458*(\varepsilon'_{\omega/16} - \varepsilon'_{16\omega}) \quad \text{(A.1)}$$

After calculation of $\varepsilon''(\omega)$, we move the $\Sigma\varepsilon'$-window step by step up and down the ω-scale in order to calculate $\varepsilon''(2\omega), \varepsilon''(4\omega), \ldots$ and $\varepsilon''(\omega/2), \varepsilon''(\omega/4), \ldots$ respectively. The use of (A.1) can be continued until we reach the edges of the frequency range. We then change over to the special sets of coefficients listed in Table 1 which we apply in combination with Eqs. (7) or (8).

Calculation of the Ohmic conductivity

Note that the calculation of the Ohmic conductivity using ε''_{KK} for ε''_{rel} in Eq. 12 is more universal and more accurate than fitting ε''_{rel} to an empirical equation, such as that of Havriliak and Negami, as is often done. This more common approach has in fact three deficiencies.

First, one can question whether the underlying relaxations really obey the Havriliak–Negami equation. This will certainly not be true when the contributions of interfacial or space-charge relaxations are strong.

Another drawback is that a direct fit of the measured ε''-data to:

$$\varepsilon''(\omega, T) = \mathrm{Im}\left(\frac{\varepsilon_s - \varepsilon_\infty}{(1 + \{i\omega\tau(T)\}^b)^a}\right) + \frac{\sigma_{dc}(T)}{\varepsilon_v \omega} \quad \text{(A.2)}$$

is rather ill-posed, so that all the parameters, and thus $\sigma_{dc}(T)$, cannot be calculated accurately. The same applies to a Havriliak–Negami fit to the ε'-data.

Finally, such fitting procedures are much more elaborate than the calculation of ε''_{KK} from ε'. The more so, because they are non-linear and have to be repeated for every measuring temperature.

Appendix 2

A HP-Basic program for performing the numerical Kramers-Kronig conversion.

```
 10 ! ************************************************
 20 ! PROGRAM KKCONV: numerical Kramers-Kronig Conversion
 30 ! ************************************************
 40 ! Variable Np contains the number of frequencies, which differ
 50 ! by a factor 2.
 60 ! Array's Eps1 and Eps2 contain the real and imaginary part of
 70 ! the dielectric constant
 80 ! = = = = = = = = = = = = = = = = = = = = = = = = = = = = = = = =
 90 COMPLEX Ep
100 INTEGER I, J, Np, Nt, N0, N1, N2
110 REAL U(1:4, 1:4), W(1:4, 1:4), A, B, Fs
120 Np = 17
130 N0 = (Np + 1)/2
140 N1 = N0 - 1
150 N2 = N0 + 1
160 ALLOCATE Eps1(1:Np), Eps2(1:Np), Wt(1:Np)
170 ALLOCATE H(1:Np), R(1:Np), Eps2kk1(1:Np), Eps2kk2(1:Np)
180 ! ------------------
190 ! READ COEFFICIENTS
200 ! ------------------
210 DATA 1.08161, 0.08725, 0.92852, 0.44530
220 DATA -0.64564, 0.50708, -0.42063, 0.22726
230 DATA 0.38196, -0.21489, 0.33275, -0.11000
240 DATA 0.01612, 0.15248, 0.00513, 0.13458
250 READ U(*)
260 DATA 0, 0.42660, 0.46975, 0.50888
270 DATA 0, -0.10012, -0.13497, -0.17575
280 DATA 0, -0.00214, 0.00888, 0.02853
```

```
290 DATA 0, 0.00123, -0.00015, -0.00417
300 READ W(*)
310 ! = = = = = = = = = = = = = = = = = = = = = =
320 ! Generate Eps' and Eps'' data for test purposes
330 ! = = = = = = = = = = = = = = = = = = = = = =
340 Fs = 1
350 A = .6
360 B = 2^(-N0)
370 ! Cole-Cole equation
380 FOR I = 1 TO Np
390   B = 2*B
400   Wt(I) = B
410   Ep = 1/(1 + (CMPLX(0, 1)*Fs*B)^A)
420   Eps1(I) = 1 + REAL(Ep)
430   Eps2(I) = -IMAG(Ep)
440 NEXT I
450 ! = = = = = = = = = = = = = = = = = = = = = =
460 ! PERFORM KK-TRANSFORMATION
470 ! = = = = = = = = = = = = = = = = = = = = = =
480 ! ------------------------------------------------
490 ! Solve equations (3), (7) and (8) for calc. Eps'' from Eps'
500 ! ------------------------------------------------
510 FOR I = 2 TO Np-1
520   SELECT I
530   CASE 2, 3, 4
540     Nt = I - 1
550   CASE Np-3, Np-2, Np-1
560     Nt = Np - I
570   CASE ELSE
580     Nt = 4
590   END SELECT
600   Eps2kk1(I) = 0
610   H(I) = 0
620   FOR J = 1 TO Nt
630     B = Eps1(I-J) - Eps1(I + J)
640     Eps2kk1(I) = Eps2kk1(I) + U(J, Nt)*B
650     H(I) = H(I) + W(J, Nt)*B
660   NEXT J
670   SELECT I
680   CASE < Np/2
690     FOR J = Nt + 1 TO 4
700       B = Eps1(I) - Eps1(I + J)
710       Eps2kk1(I) = Eps2kk1(I) + U(J, Nt)*B
720       H(I) = H(I) + W(J, Nt)*B
730     NEXT J
740   CASE > Np/2
750     FOR J = Nt + 1 TO 4
760       B = Eps1(I - J) - Eps1(I)
770       Eps2kk1(I) = Eps2kk1(I) + U(J, Nt)*B
780       H(I) = H(I) + W(J, Nt)*B
790     NEXT J
800   END SELECT
```

```
 810 NEXT I
 820 MAT R = Eps2kk1
 830 MAT Eps2kk2 = Eps2kk1
 840 ! ----------------------------------------------
 850 ! First iteration for optimizing calc Eps" from Eps'
 860 ! using equation (10)
 870 ! ----------------------------------------------
 880 FOR I = N2 TO Np-2
 890   R(I) = .4*(R(I - 1) + Eps2kk1(I + 1)) + H(I)
 900 NEXT I
 910 FOR I = N1 to 3 STEP - 1
 920   R(I) = .4*(Eps2kk1(I - 1) + R(I + 1)) + H(I)
 930 NEXT I
 940 I = N0
 950 R(I) = .4*(R(I - 1) + R(I + 1)) + H(I)
 960 ! ----------------------------------------------
 970 ! Second iteration for optimizing calc Eps" from Eps'
 980 ! using equation (10)
 990 ! ----------------------------------------------
1000 FOR I = N2 TO Np-2
1010   Eps2kk2(I) = .4*(Eps2kk2(I - 1) + R(I + 1)) + H(I)
1020 NEXT I
1030 FOR I = N1 to 3 STEP - 1
1040   Eps2kk2(I) = .4*(R(I - 1) + Eps2kk2(I + 1)) + H(I)
1050 NEXT I
1060 I = N0
1070 Eps2kk2(I) = .4*(Eps2kk2(I - 1) + Eps2kk2(I + 1)) + H(I)
1080 ! -------------
1090 ! Print results
1100 ! -------------
1110 ! PRINT USING "7A, Z.DD";"ALPHA = ",A
1120 ! PRINT USING "12A, DDD.DD";"FREQ-SHIFT = ",Fs
1130 PRINT
1140 PRINT "OMEGA *TAU EPS1CC EPS2CC EPS2KK1 EPS2KK2"
1150 FOR I = 1 TO Np
1160   PRINT USING "MD.DDESZZ,3X,4(MZ.DDD,3X)";Wt(I), Eps1(I), Eps2(I), Eps2kk1(I), Eps2kk2(I)
1170 NEXT I
1180 ! -------------
1190 ! Print to file
1200 ! -------------
1210 File$ = "output"
1220 CREATE File$, 1
1230 ASSIGN @Datafile TO File$
1240 FOR I = 2 TO Np - 1
1250   OUTPUT @Datafile USING "MD.DDESZZ,A,3(MZ.DDDD,A)";Wt(I),
       ",", Eps2(I), ",", Eps2kk1(I), ",", Eps2kk2(I)," "
1260 NEXT I
1270 ASSIGN @Datafile TO *
1280 END
```

References

1. Maxwell JC (1892) Electricity and Magnetism, Vol 1
2. Wagner KW (1914) Arch Elektrotech 2:378
3. Sillars RW (1937) J Inst Electr Eng 80:378–394
4. van Beek LKH (1967) Progress in Dielectrics 7:69–114
5. Bánhegyi G (1986) Colloid Polym Sci 264:1030–1050
6. Steeman PAM (1992) PhD-Thesis Delft University of Technology
7. Köhler W et al (1991) Macromolecules 24:4589–4599
8. Vallerien SU et al (1990) Liquid Crystals 8:719–725
9. Rellick GS, Runt J (1986) J Polym Sci Polym Phys Ed 24:279–302
10. Brather A (1979) Colloid Polym Sci 257:467–477
11. Schwarzl FR (1970) Rheol Acta 9:382 (1971) Rheol Acta 10:166 (1975) Rheol Acta 14:581
12. Ferry JD (1960) Viscoelastic Properties of Polymers, John Wiley & Sons, Inc, New York
13. Schönhals A, Schlosser E (1989) Colloid Polym Sci 267:125–132
14. Cole KS, Cole RH (1941) J Chem Phys 9:341–351
15. Steeman PAM, Gondard C, Scherrenberg RL (1994) J Polym Sci B: Polym Phys 32:119–130